

Effects of Serum Adsorption on Cellular Uptake Profile and Consequent Impact of Titanium Dioxide Nanoparticles on Human Lung Cell Lines

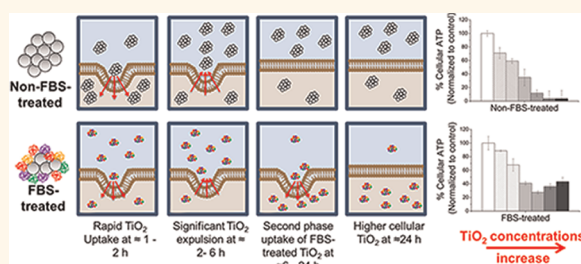
Roslyn Tedja,[†] May Lim,^{†,*} Rose Amal,[†] and Christopher Marquis^{‡,*}

[†]ARC Centre of Excellence for Functional Nanomaterials, School of Chemical Engineering, The University of New South Wales, Sydney NSW 2052, Australia and

[‡]School of Biotechnology and Biomolecular Sciences, The University of New South Wales, Sydney NSW 2052, Australia

When nanoparticles are introduced into a biological environment (such as serum), the particles may interact and adsorb protein(s) rapidly, which then alters their aggregation state, surface chemistry, and shape, leading to a new “biological identity” that is distinct from its “synthetic identity” (arising from the synthesis processes).¹ Nanosized particles have a large specific surface area, potentially with a high local charge density that can interact with biomolecules in their surrounding environment in cell culture or biological fluids.² The spontaneous adsorption of single proteins (for example, bovine or human serum albumin) or complex protein mixtures (such as in whole serum) has been shown to reduce the aggregate size of a chemically diverse range of nanoparticles, including ultrafine titanium dioxide, fullerenes, polystyrene, magnetite, tungsten carbide, ceria oxide, and zirconia nanoparticles in cell culture.^{3–9} The size of the primary particles has also been shown to be a key factor governing the adsorbed protein characteristics and the eventual size of the resulting nanoparticle aggregates.^{6,10} Interestingly, the formation of a protein layer (usually known as a protein corona) on the surface of nanoparticles has been reported to depend not only on the primary size of particles but also on the type of suspending media. Roswell Park Memorial Institute medium (RPMI) supplemented with fetal bovine serum (FBS) has been noted to significantly increase the thickness of the protein layer with the increase of the primary size of gold nanoparticles, but a similar trend is not observed when Dulbecco modified Eagle’s medium (DMEM), supplemented with FBS, is used as a suspending media.¹¹ In addition, nanoparticles that

ABSTRACT



Exposure to fetal bovine serum (FBS) is shown herein to reduce the aggregate size of titanium dioxide (TiO₂) nanoparticles, affecting uptake and consequent effect on A549 and H1299 human lung cell lines. Initially, the cellular uptake of the FBS-treated TiO₂ was lower than that of non-FBS-treated TiO₂. Expulsion of particles was then observed, followed by a second phase of uptake of FBS-treated TiO₂, resulting in an increase in the cellular content of FBS-treated TiO₂, eventually exceeding the amount by cells exposed to non-FBS-treated TiO₂. Surface adsorbed vitronectin and the clathrin-mediated endocytosis pathway were shown to regulate the uptake of TiO₂ into A549 cells, while the endocytosis mechanism responsible remains elusive for H1299. Intriguingly, nystatin treatment was shown to have the unexpected effect of increasing nanoparticle uptake into the A549 cells *via* an alternate endocytic pathway. The surface adsorbed serum components were found to provide some protection from the cytotoxic effect of endocytosed TiO₂ nanoparticles.

KEYWORDS: titanium dioxide nanoparticle · serum protein · human lung cell · uptake · nanoparticle toxicity · nystatin · vitronectin

were exposed to protein molecules were also shown to adopt the physicochemical properties of the adsorbed protein shell.^{12–14} For instance, serum protein adsorption onto positively charged gold nanorods and polyethyleneamine-coated magnetite has been shown to switch their positive surface charge to negative.^{15,16}

The definite role of adsorbed protein in promoting nanoparticle uptake is not well understood, although several investigators have suggested that surface-adsorbed

* Address correspondence to
m.lim@unsw.edu.au;
c.marquis@unsw.edu.au.

Received for review February 2, 2012
and accepted April 19, 2012.

Published online April 20, 2012
10.1021/nn3004845

© 2012 American Chemical Society

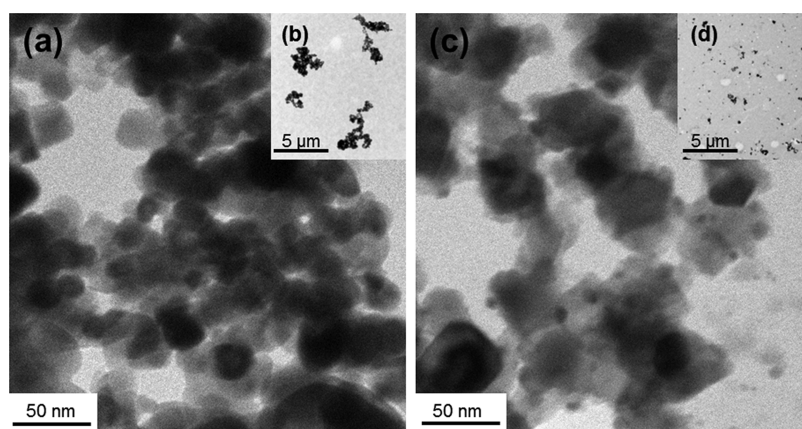


Figure 1. Transmission electron microscopy images at different magnifications of TiO_2 nanoparticles that have been incubated with (a, b) phosphate buffer solution (PBS, as non-FBS-treated particle) or (c, d) fetal bovine serum (FBS, as FBS-treated particle) for 15 h and then resuspended in serum-free RPMI1640 media supplemented with 1% L-glutamine.

proteins promote nanoparticle uptake *via* receptor-mediated endocytosis.^{5,16,17} It has been demonstrated that the nanoparticle–cell association did not depend on the identity of the adsorbed proteins, but rather on the capacity of the surfaces to bind protein.¹⁸ To some extent, this confirms the observation of other investigators who found that the amount of nanoparticles taken up is proportional to the amount of adsorbed protein.¹⁹ Conversely, a reduction in the uptake of magnetite, carbon, and gold nanorods,¹⁷ and no effect on the internalization of anionic mesoporous silica nanoparticles by macrophages cells,²⁰ was observed after protein modification of the nanoparticles' surface. It has also been shown that there is no difference in the uptake of nanoparticles with different surface functionalization (*i.e.*, COOH, NH_2 , or polyethylene glycol) after the nanoparticles have been exposed to serum for several hours.²¹

Serum protein induced changes in the physicochemical characteristics, and cellular uptake is expected to alter the nanoparticle's biological impact. Nonetheless, the literature is scarce and inconclusive with regard to precisely how serum protein adsorption influences the outcome of the toxicity assessment. It has been shown that the use of a poloxamer surfactant (Pluronic F127) to disperse single-walled carbon nanotubes and amorphous silica resulted in a significant loss of protein binding and, subsequently, a lower toxicity effect of the nanoparticles toward the RAW 264.7 macrophage-like cell line.²² The toxicity of cadmium ions originating from CdSe nanoparticles has been reported to be reduced significantly for a number of cell lines in serum-free media.²³ Gold nanorods were shown to exhibit lower toxicity toward human cervical cancer cells (HeLa cells) *in vitro* when serum-containing media was used in the cell culture; this was attributed to the lower uptake of the gold nanorods in the presence of serum.²⁴ Similarly, the reactive oxygen species (ROS) response from the Monomac-6 cell line that was exposed

to carbon black particles was reduced when cell culture media containing bovine serum albumin was used in the assay.⁴ In contrast, Sager *et al.* (2007) showed silica suspended in broncho-alveolar lavage fluid produced similar levels of pulmonary inflammation and lactate dehydrogenase release by A549 lung cells to silica suspended in phosphate buffer solution.²⁵ Clift *et al.* (2010) measured the cytotoxic response, intracellular glutathione (GSH) levels, and tumor necrosis factor- α production of J774.A1 murine “macrophage-like” cells upon exposure to 20 and 200 nm polystyrene nanoparticles. They showed that the smaller nanoparticles were equally toxic regardless of whether the media contained serum or not, whereas larger nanoparticles suspended in serum-containing media were less toxic than particles of the same size suspended in serum-free media.²⁶

A holistic approach is applied herein to investigate the effects of serum protein adsorption on the aggregate size and cellular interactions of titanium dioxide (TiO_2), a commercially relevant and widely used nanomaterial, that has been exposed to FBS. The uptake of FBS- and non-FBS-treated TiO_2 into two different human lung cell lines (A549 and H1299) was investigated *in vitro* from a kinetic and mechanistic perspective. The cellular particle uptake mechanism(s) was also elucidated using temperature shift and chemical inhibition experiments. The effect of vitronectin attachment, an abundant glycoprotein component of serum, on cellular uptake was also investigated. Cell counts and *in vitro* toxicity assays were then used to quantify the degree of biological impact of the serum-treated nanoparticles.

RESULTS AND DISCUSSION

Effects of Serum Protein Adsorption on the Aggregation Stability of TiO_2 Nanoparticles in Cell Culture Media. Figure 1 shows typical transmission electron microscopy (TEM) images of TiO_2 nanoparticles that have been exposed to phosphate buffer solution (PBS, non-FBS-treated TiO_2 , Figure 1a,b) or fetal bovine serum

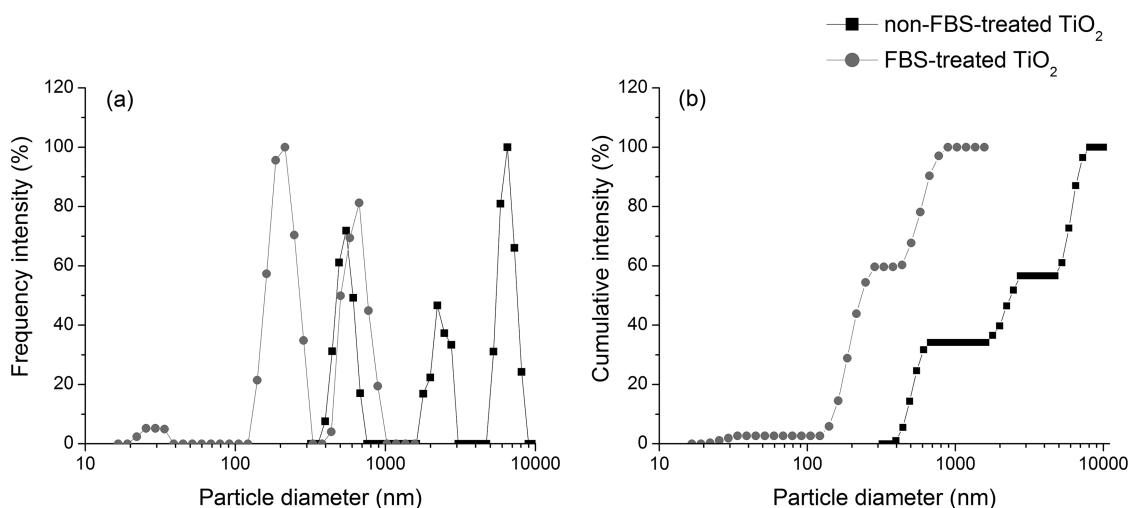


Figure 2. Particle size distribution of non-FBS-treated and FBS-treated TiO₂ suspended in RPMI1640 cell culture media supplemented with 1% L-glutamine based only on (a) frequency intensity and (b) cumulative intensity.

(FBS, FBS-treated TiO₂, Figure 1c,d) for a period of 15 h and then resuspended in serum-free culture media. At high magnification, it can be seen that FBS-treated TiO₂ has a layer of gelatinous substance on the surface of TiO₂ particles (Figure 1c). This layer was not seen on the surface of non-FBS-treated TiO₂ (Figure 1a). The aggregate size of the FBS-treated TiO₂ nanoparticles in cell culture media is also smaller (Figure 1d), and dynamic light scattering (DLS) size measurements confirm that the aggregates are in the nano size range (Figure 2). Conversely, both TEM imaging (Figure 1b) and DLS analysis (Figure 2) show non-FBS-treated TiO₂ nanoparticles exist as a mixture of submicrometer and micrometer-sized aggregates in cell culture media. It is noted here that particle size in the micrometer range measured by DLS is only indicative, as the upper detection limit of the Brookhaven 90Plus instrument is 6 μm .

The layer of gelatinous substance on the surface of TiO₂ particles is a complex mixture of adsorbed serum components including proteins; a similar coating of nanoparticles has been observed previously for TiO₂, as well as fullerenes, gold, polystyrene, and magnetite nanoparticles that have been exposed to proteins.^{5,7,9,24,27} Deguchi *et al.* (2007) showed that the adsorbed proteins reduce nanoparticle aggregation by forming a steric layer on the particle surface, which prevents salt-induced aggregation.⁵ Wiogo *et al.* (2011) further showed that strongly adsorbed protein molecules serve as linkers that aid the adsorption of proteins with lower affinities for the nanoparticle surface; it is the low-affinity proteins, however, that provide the required steric hindrance.⁷ It is likely that similar adsorption and stabilization mechanisms are involved here. Non-FBS-treated TiO₂ nanoparticles that were suspended in serum-free media, on the other hand, aggregated rapidly due to shielding of their electrostatic layer by salt ions such as NaCl, KCl, Na₂H₂PO₄, and Na₂HPO₄ that are present in the media.²⁸

Effects of Protein Adsorption on the Uptake of TiO₂ Nanoparticle into Human Lung Cell Lines.

The cell counts and the amount of non-FBS-treated and FBS-treated TiO₂ taken up into A549 and H1299 cells after 24 h of particle exposures are shown in Figure 3. For A549 cells, the uptakes of both FBS- and non-FBS-treated TiO₂ are dose dependent and similar until the particle concentration reaches 2000 $\mu\text{g}/\text{mL}$. At a concentration of 2000 $\mu\text{g}/\text{mL}$ or greater, the amount of FBS-treated TiO₂ taken up into A549 cells increased dramatically to the point of cell saturation; this did not occur with non-FBS-treated TiO₂. For H1299 cells, the amount of FBS-treated TiO₂ taken up by the cells is more than twice that of non-FBS-treated TiO₂. Moreover, the same amounts of FBS-treated TiO₂ (maximum cellular capacity of approximately 2300 pg/cell) were taken up into H1299 cells for the range of TiO₂ dose studied. Contact with serum, which reduces the size of the TiO₂ aggregates, is shown to also increase the amount of particles taken up into both cell lines when measured at 24 h. This contrasts with our previous findings, which showed the same cells had a lower particle uptake when exposed to sonicated TiO₂ (which reduces the aggregate size) than when they were exposed to larger nonsonicated aggregates.²⁹

The data also show that cells that were not exposed to TiO₂ nanoparticles increased from the initial seeded density of 1.6×10^5 cells to about 4.5×10^5 cells in wells with 9.6 cm² culturable surface area after 24 h. As anticipated, cells that were exposed to TiO₂ exhibited a lower cell count than the unexposed (control) cells. The cell count decreases with increases in particle concentration; at high particle concentration, the cell count dropped below its initial value. Hoechst stain (Hoechst 33342 dye, 1.0 mM) further confirms the observed drop in cell count is due to impairment of cell growth and/or viability caused by particle exposure and not by the washing steps (see Supporting Information). What is

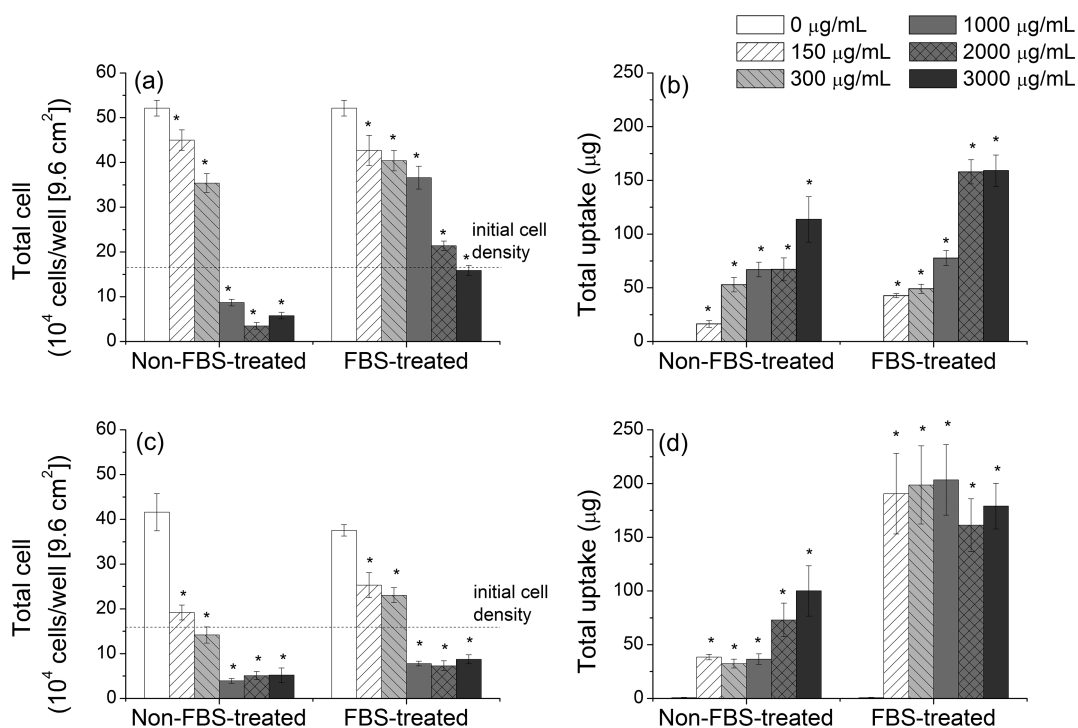


Figure 3. Number of cells (left) and amount of particles taken up (right) by A549 (top) and H1299 (bottom) cell lines after 24 h of exposure to non-FBS-treated and FBS-treated TiO₂ nanoparticles. Groups significantly different from the untreated group (marked as 0 µg/mL) (by one-way ANOVA followed by Dunnett's test) are shown by **p* < 0.05, from at least 5 independent experiments.

unexpected is cells that were exposed to FBS-treated TiO₂ had a higher cell count than cells that were exposed to non-FBS-treated TiO₂, despite the fact that more FBS-treated TiO₂ particles were taken up into the cells. These results again contrast with our previous findings, and that of several others, which showed higher particle uptake generally results in lower cell viability and growth rates.²⁹

To further explain the observed cell count and particle uptake results, the amount of non-FBS- and FBS-treated particles taken up by A549 and H1299 cell lines in a 24 h period after exposure to 150 µg/mL of TiO₂ was measured, and the results are shown in Figure 4. The data highlights several interesting effects of serum adsorption on the uptake of nanoparticles into biological cells, and to the best of our knowledge, some of these observations have not been reported in the literature.

First, a rapid uptake of particles at the initial stage of exposure was observed for both cell lines. For FBS-treated TiO₂ particles, the amount taken up initially is lower; approximately half of that of non-FBS-treated TiO₂. The higher uptake of non-FBS-treated TiO₂ at the initial stage of exposure can be attributed to its larger aggregate size (compared to FBS-treated TiO₂). It has previously been shown that larger aggregates will sediment more rapidly onto the adhered cells, subsequently exposing the adhered cells to higher localized concentrations of particles.^{29,30}

Second, as much as 30% to 40% of the TiO₂ particles that were taken up by A549 and H1299 were expelled by the cells (exocytosis) within 2 h after exposure, resulting in a significant drop in the cellular TiO₂ content. The cellular content of FBS-treated TiO₂ in A549 cells remained relatively steady in the period after particle expulsion, whereas that of H1299 cells continued to increase before decreasing again at 10 h. For non-FBS-treated TiO₂, the cellular content decreases steadily once expulsion occurs. Similarly, exocytosis of polysaccharide-coated nanoparticles by 16HBE14o airway epithelium cells after 30 min of exposure has been reported previously.³¹ Exocytosis of foreign material is a dynamic cellular process, in which the internalized membrane and compartments are continuously recycled to the cell surface. The rapid decrease, followed by a gradual decrease in intracellular particles over a 24 h period following exposure, suggests that at least two intracellular compartments could be involved: (i) one that turns over rapidly and (ii) one that turns over relatively slowly.³² The particle fraction that were going to the recycling endosomes, which have a fast turnover rate, may be exocytosed rapidly, while those particles that escaped the recycling endosome into the cytoplasm or lysosomes with a slower turnover rate were exocytosed from the cells more slowly.

Third, a second phase of particle uptake was observed for FBS-treated TiO₂ sometime after 6 to 12 h of particle exposure for both A549 and H1299 cells.

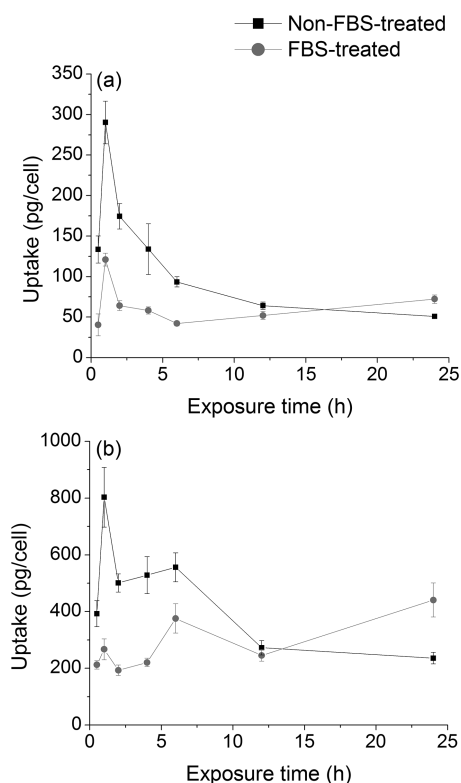


Figure 4. Kinetic cellular uptake of non-FBS-treated and FBS-treated TiO₂ particles by (a) A549 and (b) H1299 cell lines during 24 h period of exposure, from at least 3 independent experiments.

The consequence of this is at 24 h after particle exposure, the amount of FBS-treated TiO₂ in both A549 and H1299 cells is greater than that of non-FBS-treated TiO₂ in the same cells. This later stage uptake of particles was not observed for cells exposed to non-FBS-treated TiO₂. The effect of serum treatment resulting in increased total particle uptake at 24 h is consistent with the uptake data shown in Figure 3 and later in Figure 6.

Fourth, there is a difference in the amount of TiO₂ particles taken up by A549 and H1299 under the same experimental conditions. The difference in uptake can also be attributed to the distinct characteristics of the two cell lines, including (1) mutation of p53 oncogene repressor on H1299 cells and (2) that A549 produces large amounts of lecithin, which is known to contribute to phospholipid biosynthesis and therefore possibly result in altered membrane structure and fluidity compared to H1299.²⁹

Insights into the Mechanisms of Particle Uptake by Human Lung Cell Lines. The uptake results clearly indicate that the nonspecific adsorption of serum components onto the TiO₂ surface strongly influences their interaction with the cells and can potentially change the mechanism of cellular entry and thereby the extent and rate of particle uptake. To further investigate this, the uptake mechanism and pathway and the role of vitronectin (a cell adhesion protein component of serum) on the uptake process were determined.

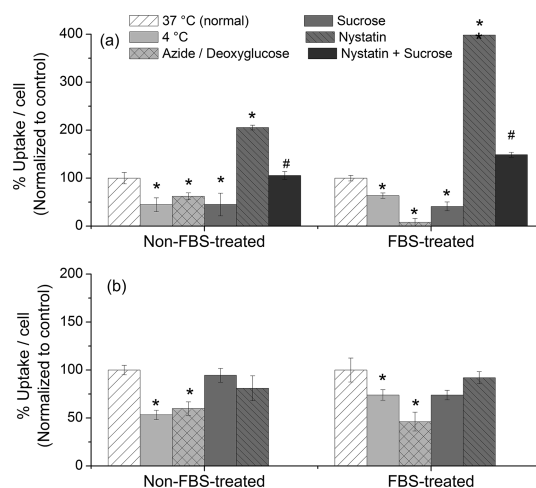


Figure 5. Total amount of non-FBS-treated and FBS-treated TiO₂ nanoparticle that were taken up into (a) A549 and (b) H1299 cells after 1 h of exposure to 150 μg/mL of particles, under four different treatments that are known to be inhibitory to cellular uptake, namely, low temperature (4 °C), ATP depleted (azide/deoxyglucose), caveolae disruption (nystatin), and hypertonic (sucrose). For A549 cells, a combination of nystatin and sucrose treatment was also applied (nystatin+sucrose). Groups significantly different from the control group (37 °C normal) and nystatin-treated group (by one-way ANOVA followed by Dunnett's test) are shown by **p* < 0.05 and #*p* < 0.05, from at least 3 independent experiments.

The cellular uptake mechanism(s) of non-FBS- and FBS-treated TiO₂ into A549 and H1299 cells can be revealed to some extent by subjecting the cells to treatments that are inhibitory to cellular uptake.¹⁶ In the present work, the following treatments were applied: (1) low temperature (incubated at 4 °C), (2) adenosine triphosphate (ATP) depletion (azide/deoxyglucose), (3) caveolae disruption by cholesterol sequestration (nystatin), and (4) hypertonic treatment (sucrose). In this study, both the growth and viability of A549 and H1299 cell lines were shown to be unaffected by these treatments for a total period of 2 h (see Supporting Information). Cells incubated with non-FBS-treated or FBS-treated TiO₂ nanoparticles at 37 °C and without any inhibitors are identified as "normal" in the same figure. Following treatment, the cells were exposed to particles for 1 h, the period where the net cellular uptake of particles was at its maximum.

Figure 5 shows the amount of non-FBS-treated and FBS-treated TiO₂ nanoparticles that were taken up by the cells after the inhibitory treatments. For both A549 and H1299 cells, the amount of non-FBS-treated and FBS-treated TiO₂ nanoparticles taken up was reduced relative to the normal conditions (37 °C) when the cells were incubated at 4 °C. This decrease in particle uptake is attributed to the significant reduction of available cellular energy at 4 °C, which diminishes energy-dependent endocytosis. This is further confirmed by the significant reduction in the amount of particles taken up by the two cell lines after incubation with

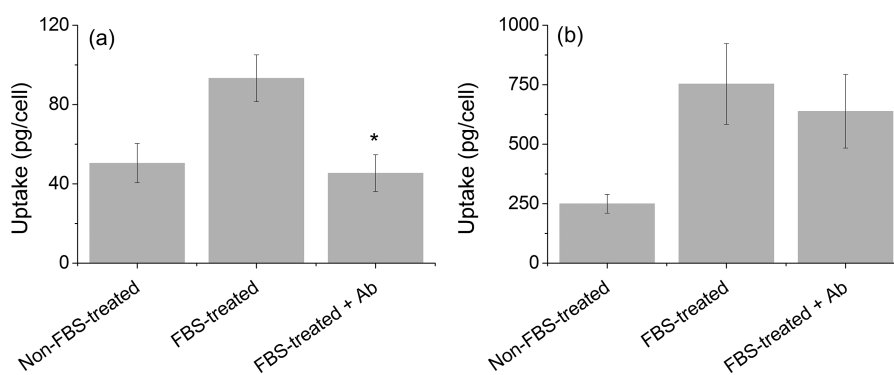


Figure 6. Amount of particles taken up by (a) A549 and (b) H1299 cell lines after 24 h of exposure to 150 $\mu\text{g/mL}$ of TiO_2 nanoparticles that were treated with phosphate buffer solution (non-FBS-treated), fetal bovine serum (FBS-treated), and fetal bovine serum followed by anti-vitronectin antibody incubation (FBS-treated + Ab). Groups significantly different from the group that was treated with FBS-treated particle (by one-way ANOVA followed by Dunnett's test) are shown by * $p < 0.05$, from at least 3 independent experiments.

sodium azide and deoxyglucose. Sodium azide inhibits the cellular oxidative respiration by blocking cytochrome *c* oxidase (the last enzyme in the mitochondrial electron transport chain), thereby limiting the production of cellular ATP energy.^{33,34} The fact that the cellular uptake of TiO_2 particles is reduced at low temperature and in ATP-depleted environments established that endocytosis, an energy-dependent process that requires the cell membrane wall to flex and bulge inward, is one of the main portals for TiO_2 particle entry into both A549 and H1299 cells.

To further verify which type of endocytosis mechanisms are responsible for TiO_2 particle uptake, the cells were incubated in a hypertonic environment (induced by adding sucrose) or exposed to nystatin (a cholesterol sequestration agent). A hypertonic condition will cause water to diffuse out from the cells, thereby disrupting the formation of clathrin lattice in the cell membrane.³⁵ The drop in the amount of nanoparticles taken up by A549 cells under a hypertonic condition suggests that the endocytosis of TiO_2 particles into the cells occurs *via* a clathrin-mediated pathway.

Interestingly, when A549 cells were exposed to nystatin, no inhibitory effect on the uptake of TiO_2 nanoparticles into the cells was observed. In fact, the amount of nanoparticles taken up doubled and tripled for non-FBS- and FBS-treated TiO_2 , respectively, compared to "normal" levels. Nystatin is known to disrupt caveolae/lipid raft formation in the membrane of fibroblasts³⁶ and endothelial cells³⁷ without affecting the clathrin lattice; it is also known to inhibit macropinocytosis.³⁸ The fact that the uptake of nanoparticles by A549 cells was enhanced when under nystatin treatment suggests that the blocking of caveolae-mediated and macropinocytosis pathways up-regulates other uptake pathways. Moreover, simultaneous treatment of the cells with a combination of sucrose and nystatin caused the amount of TiO_2 nanoparticles taken up to revert back to a level that is similar

to the control (37 °C). This suggests that when macropinocytosis and low-efficiency caveolae/lipid rafts were blocked in A549 cells, the high-efficiency clathrin-mediated pathway is one of the pathways that was upregulated. The promoting effect of nystatin has also been observed in the uptake of endostatin into primary HUVEC endothelial cells and human microvascular endothelial cells, but paradoxically not into A549 cells.³⁹ Others have observed that the disruption of caveolae/lipid rafts with cholesterol-sequestering agent can trigger displacement of prion protein from lipid rafts into a clathrin-mediated machinery, thereby elevating endocytosis of the protein into a human neuroblastoma cell line.⁴⁰ It is expected that a similar mechanism is at play here.

The incubation of H1299 with sucrose or with nystatin, on the other hand, made little difference in the uptake of the nanoparticles. This indicates that endocytosis of TiO_2 nanoparticles into H1299 cells occurs *via* a clathrin- and caveolae-independent pathway; however, the actual uptake mechanism remains elusive.

The effect of vitronectin protein adsorption on nanoparticle uptake was also investigated in this work. Vitronectin, an abundant glycoprotein found in serum and the extracellular matrix of many cellular systems, has been associated with cellular adhesion to surfaces.⁴¹ It has also been implicated in the uptake of crocidolite asbestos into rabbit pleural mesothelial cells⁴² and A549 cells⁴³ *via* the $\alpha_v\beta_5$ integrin receptor. The presence of vitronectin on the TiO_2 surface after the FBS treatment was confirmed by one-dimensional SDS-PAGE gel protein electrophoresis followed by Western blot (see Supporting Information). Treating the particles with antibody blocks the interaction between vitronectin on the particle surface and associated cell surface receptors.

Figure 6 shows the amount of particles taken up by A549 and H1299 cell lines after 24 h of exposure to 150 $\mu\text{g/mL}$ of non-FBS- and FBS-treated TiO_2 , as well as

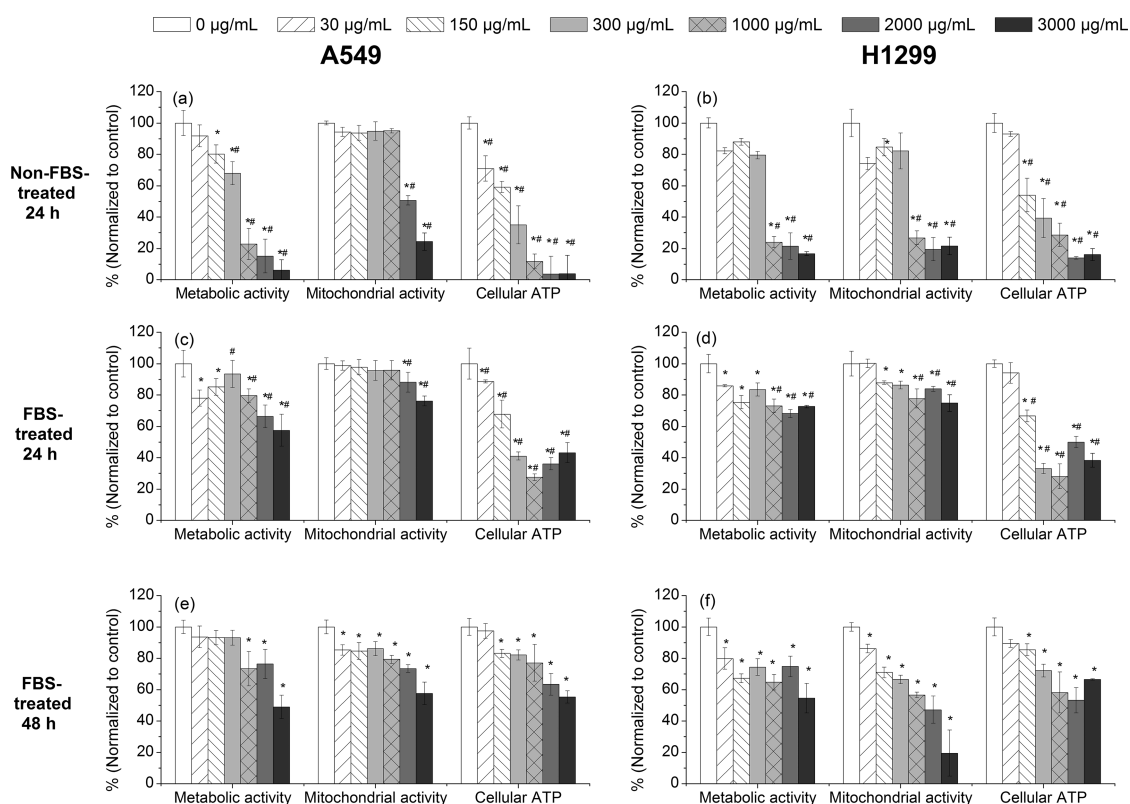


Figure 7. Metabolic activity, mitochondrial activity, and cellular ATP levels of (a, c, e) A549 and (b, d, f) H1299 cells after (a–d) 24 and (e and f) 48 h of exposure period to different concentrations of TiO₂ nanoparticles that were treated with (a and b) phosphate buffer solution or (c–f) fetal bovine serum. Groups significantly different from the control group (by one-way ANOVA followed by Dunnett's test) are shown by * $p < 0.05$. Groups significantly different from the same concentration with different FBS treatment (by one-way ANOVA followed by Dunnett's test) are shown by # $p < 0.05$, from at least 6 independent experiments.

FBS-treated TiO₂ that has been contacted with anti-vitronectin antibody. After treatment with the antibody, the amount of FBS-treated TiO₂ taken up into A549 cells was reduced by as much as 50%, and the amount of particles taken up is similar to that of non-FBS-treated TiO₂ nanoparticles. This observation indicates that the later phase of FBS-treated TiO₂ uptake into A549 cells occurs *via* an endocytosis pathway that is mediated by the binding of adsorbed proteins such as vitronectin with cell surface receptors. This is in agreement with the results of others who have shown that the coating of asbestos fibers with vitronectin enhanced its uptake into A549 lung cells through interaction with $\alpha_v\beta_5$ integrin receptors on the cells' surface.⁴³

For H1299 cells, the amount of FBS-treated TiO₂ nanoparticles taken up by the cells is similar, regardless of whether the nanoparticles have been treated previously with anti-vitronectin antibody or not. The amount of nanoparticles taken up in both cases is also greater than that of the non-FBS-treated TiO₂ (Figure 6b). Therefore, it can be concluded that vitronectin is not one of the serum proteins that can enhance the uptake of TiO₂ into H1299 cells. This may be explained by our observation that the particle uptake pathway by H1299 is different compared to A549. Our data show that uptake by H1299 involves a

caveolae- and clathrin-independent pathway, which does not require special interaction between vitronectin and an integrin receptor in order for endocytosis to occur. The attachment of biomolecules other than proteins (for example lipids) may also affect the amount and rate of particles taken up by the cells. Depending on surface charge densities, gold nanoparticles directly interact with lipid membranes, enhancing internalization of the particles.⁴⁴

Effects of Serum Protein Adsorption on the Biological Impact of TiO₂ Nanoparticles. Figure 7a–d shows a reduction in the cellular metabolic and mitochondrial activities and cellular ATP level of A549 and H1299, following a 24 h period of exposure to non-FBS- and FBS-treated TiO₂. The cellular ATP level is the parameter most affected by TiO₂ loading after 24 h. These observations are in agreement with previous investigations into the biological impact of TiO₂ on these human lung cell lines.²⁹ Our data shows that two different cell lines, A549 and H1299, that originated from the same organ (*i.e.*, human lung) may have different biological responses toward TiO₂ nanoparticles. Similarly, previous reports have suggested that the choice of target cells *in vitro* may impact the resulting assessment of toxicity of nanoparticles.^{29,45} For example, the human brain cell line BE-2-C has been reported to be more sensitive to

supramagnetic iron oxide nanoparticles compared to the human heart cell line HCM and human kidney cell line 293T under the same conditions of exposure.⁴⁵ Together with our results, published data support the “cell vision” postulation, which refers to the importance of the first contact point of the nanomaterial surface with the cells in determining the level of biological impact. This first contact point is the cell membrane, which differs in structure and composition (including the composition of surface proteins, sugars, and phospholipids) between different cells.⁴⁶ The figure also shows that FBS-treated TiO₂ particles produce a lower biological impact in both A549 and H1299 cells than non-FBS-treated TiO₂, in agreement with cell count results. The last finding is intriguing, more so because the total uptake of FBS-treated TiO₂ into the lung cells was equal, if not higher, than that of the untreated control after 24 h. While other investigators have attributed the lower biological impact of protein-associated gold and carbon nanoparticles to a reduction in their intracellular uptake,^{24,47} this is not the case in the present work.

The greater biological impact after 24 h exposure to non-FBS-treated TiO₂ could be due to increased structural damage to the cell membrane by the larger TiO₂ aggregates during uptake, a longer accumulative intracellular residence time of the non-FBS treated particles at 24 h, or surface-adsorbed serum providing some degree of protection to the cells. To determine whether the difference in biological impact of non-FBS- and FBS-treated TiO₂ is due to differences in the intracellular residence time of the particles, the cellular responses of the cells 48 h after exposure to FBS-treated TiO₂ were also measured such that the toxicity data would reflect an exposure level that would be equivalent to that of cells that have been exposed to high levels of FBS-treated TiO₂ for more than 24 h. Figure 7e,f shows that while the cellular metabolic and mitochondrial activities and the cellular ATP level of A549 and H1299 have dropped following 48 h of exposure to FBS-treated TiO₂, they are still higher than those of cells exposed to non-FBS-treated TiO₂ for 24 h. In fact, the cellular ATP levels of both cells at 48 h are higher than that at 24 h. The higher cellular ATP level measured following 48 h exposure can also be explained by (1) the cells having sufficient time to adapt to the particle exposure by various stress responses; (2) cell replication, which is occurring in particle-exposed cells, albeit at a slower rate compared to unexposed cells; and (3) at 24 h post-exposure, both cell lines no longer taking up the particles actively.

These data also indicate that the bound FBS components, including proteins, provide protective shielding against the toxicity effect of nanoparticles. It is likely that the surface-adsorbed proteins limit direct interaction between the nanoparticle and organelles within the cell,

thus lowering the impact of the nanoparticles on cellular function. Alternatively (or additionally), the low pH environment in late endosomes may also trigger the dissociation of ligand and receptors within the endosomes, which, in turn, detached and/or degraded the surface adsorbed serum proteins. These detached- and/or degraded-serum proteins may potentially provide essential amino acids (and other beneficial nutrients) to the cells, aiding cell growth and intracellular activities, thereby improving the mitochondrial and metabolic activities after TiO₂ exposure. The adsorption of FBS components, including proteins, may also ameliorate the competitive adsorption of other constitutional components in the cell culture media, improving bioavailability of these molecules.⁴⁷

CONCLUSION

Serum protein adsorption is found to reduce the aggregate size distribution of titanium dioxide (TiO₂) and affect the particles' interactions with A549 and H1299 human lung cell lines. Data collected over a 24 h exposure period reveal substantial differences in the dynamics and extent of cellular particle uptake. Rapid initial uptake of the particles was followed by the expulsion of a significant proportion of the particles taken up. For TiO₂ nanoparticles that have been exposed to serum proteins, a second phase of particle uptake was observed, resulting in higher cellular particle content after long periods of exposure. H1299 was found to internalize more particles than A549 cells. Endocytosis was determined to be the main uptake mechanism, although the exact endocytic pathway differed between the two cell lines. Surface-adsorbed vitronectin protein and a clathrin-mediated pathway were shown to regulate the uptake of TiO₂ into A549 cells, while the protein and the mechanism responsible for the uptake of TiO₂ into H1299 cells remain elusive. Nystatin treatment, which suppresses macropinocytosis and caveolae-mediated endocytosis, was shown to have the unexpected effect of increasing nanoparticle uptake into A549 by upregulating an alternate endocytic pathway. Cell count and cytotoxicity studies further reveal that even after the cumulative intracellular residence time has been taken into account, the biological impact of FBS-treated TiO₂ is still lower, thereby revealing the shielding properties of surface-adsorbed serum protein.

The findings presented herein have important implications for the field of nanotoxicology and nanomedicine. Due to their simplicity and low cost, *in vitro* toxicity assays such as those used in this work are widely used for screening and assessing the toxicity of nanoparticles. The predictive reliability of these assays can be improved through a better understanding of how the particles interact with serum proteins that are ever-present in biological systems (including cell culture media) and how this in turn affects

the particle uptake and toxicity over time. Insights into the mechanisms of particle uptake, including the use of a specific protein and/or compound such as nystatin to increase cellular uptake of nanoparticles,

may lead to novel routes for administering nanoparticle-based diagnostics and/or therapeutic agents to cells and to improvement in their biocompatibility.

MATERIALS AND METHODS

Materials. Roswell Park Memorial Institute-1640 (RPMI1640) cell culture medium, fetal bovine serum (FBS), phosphate buffered saline (PBS), Hank's buffered salt solution (HBSS), lithium dodecyl sulfate (LDS) buffer, trypsin/EDTA, and Trypan blue were all purchased from Gibco Invitrogen. L-Glutamine, whole molecule rabbit anti-chicken IgY, Sigma Fast BCIP/NBT tablet, and Tween-20 were purchased from Sigma Chemical Co. (St. Louis, MO, USA). Plastic culture microplates and flasks used in the experiment were supplied by Sarstedt AG & Co., Germany. CellTiter-Blue (AlamarBlue), CellTiter 96 MTS, and CellTiter-Glo Luminescent cell viability assays were purchased from Promega Co. (Madison, WI, USA). Hydrochloric acid (HCl) and hydrofluoric acid (HF) were from Ajax Finechem Pty Ltd. (Sydney, Australia). Rabbit polyclonal anti-vitronectin (Ab35109-1) was purchased from Abcam.

TiO₂ Nanoparticles. TiO₂ nanoparticles (anatase/rutile mixture, Aeroxide P25, Evonik, USA, previously known as Degussa P25) with an average primary size of 20 nm (Bickley *et al.* 1991) were used in this study. The TiO₂ nanoparticles used in this study were manufactured by the Aerosol process, by which titanium tetrachloride is subjected to hydrolysis in the vapor phase at an elevated temperature.⁴⁸ The composition of the TiO₂ sample used in this work was determined previously using X-ray diffraction (X'pert Multipurpose X-ray Diffraction System, MPD, Philips) to be 80% anatase and 20% rutile,^{29,48} and the surface area was reported to be approximately 50.0 m²/g.⁴⁸

The particles were subjected to milling using a mortar and pestle for 5 min, dispersed in PBS (pH 7.4) to a concentration of 30 mg/mL, and sterilized by autoclaving at 121 °C for 20 min. The particles were then subjected to incubation with FBS (FBS-treated) or only incubated in PBS (non-FBS-treated) overnight (15 h). The particles were washed three times with PBS to remove unattached proteins and suspended in PBS at a concentration of 30 mg/mL. The TiO₂ stock solution was diluted with RPMI1640 media supplemented with 1% (w/v) L-glutamine (without any further FBS supplement) prior to characterization of particle size distribution and cell exposure to TiO₂ particles.

Particle Size Distribution Characterization. The sizes of the non-FBS- and FBS-treated TiO₂ aggregates were characterized using dynamic light scattering (Nano-DLS, Brookhaven) at 37 °C (temperature at which cell culture was conducted) and transmission electron microscopy (JEOL1400, operating at 100 kV). The non-FBS- and FBS-treated particles were dispersed in the RPMI1640 media supplemented with 1% L-glutamine (no FBS).

One-Dimensional Gel Electrophoresis. The proteins adsorbed onto FBS-treated and control particles were extracted by incubating the particles with 100 μL of LDS sample loading buffer for 30 min. The sample was then diluted at ratios of 1:5, 1:10, 1:20, and 1:40 with LDS buffer followed by incubation at 95 °C for 10 min. The protein extracts were loaded onto NuPAGE Novex 4–12% Bis-Tris gel and 2-(N-morpholino)ethane sulfonic acid as the running buffer. A constant voltage of 170 V for 45 min was applied to separate the protein mixture based on its molecular weight. The gels were then either used for Western blotting or fixed with 10% acetic acid, 50% methanol, and 40% water (v/v) for 15 min. The fixed gel was then stained by using Gel Code Blue stain solution overnight followed by destaining with water for approximately 1 h.

Western Blot Specific to Vitronectin Protein. Proteins separated using one-dimensional gels were transferred by a semidry technique (Hoefer Semi-Dry Transfer Unit, Hoefer) onto nitrocellulose membranes with 25 mM Tris, 250 mM glycine, and 20% (v/v) methanol as the transfer buffer. A constant current of 2 mA/cm² was then applied for 3.5 h to achieve a complete protein transfer.

The transferred proteins on the membrane were blocked with blocking solution (4% (w/v) skim milk in PBS) overnight. The membrane was then washed three times with PBS (5 min each). The membrane was immersed in 1:1000 rabbit polyclonal anti-vitronectin (specific to bovine vitronectin) antibody in PBS incubated at room temperature with rocking for 1.5 h. The membrane was washed twice with PBS (5 min each) followed by PBS-T (PBS buffer added with 0.1% (v/v) Tween 20). The membranes were then soaked in secondary antibody (whole molecule chicken IgY anti-rabbit antibody) at a 1:10000 dilution in PBS and incubated for 1 h. The membrane was again washed twice with PBS (5 min each) followed by PBS-T (PBS buffer added with 0.1% (v/v) Tween 20). The membrane was stained using 10 mL of Sigma Fast BCIP/NBT solution for 5–10 min and destained with water.

Cell Lines. Human lung epithelial cell lines, A549 (ATCC, CCL-185) and NCI-H1299 (ATCC, CRL-5803), kindly provided by Dr. Louise Lutze-Mann, were separately cultured in RPMI1640 media supplemented with 10% FBS and 1% L-glutamine. The cells were cultured in treated T75 flasks and incubated at 37 °C in a humidified incubator with a 5% CO₂ atmosphere (Heraeus). Cell culture experiments were performed in 96-well treated-culture plates for the biological assays (AlamarBlue, MTS, and ATP luminescent assays) and six-well treated-culture plates for the viable cell count by Trypan blue assay and quantification of particle uptake. Cells were generally seeded with an initial density of 1.6×10^4 cells/cm² into the tissue culture flasks or plates 15–16 h prior to particle exposure.

Particle Uptake Measurement. After 24 h incubation with TiO₂ particles at concentrations between 150 and 3000 μg/mL, the cell media was removed and the cells were washed three times with HBSS to remove the noninternalized particles. The cells were then incubated with 1 mL of 6 M HCl overnight. The entire contents of the well were retrieved, and each well was washed three times with 1 mL of Milli-Q water. The combined HCl extract together with the washes was treated with 1 mL of 40% (w/w) HF and incubated overnight at room temperature. The samples were then diluted to a final volume of 10 mL with Milli-Q water, and the Ti contents were quantified using ICP-OES (PerkinElmer Optima, 3000DV).

Cellular Uptake Inhibition Study. To study the mechanism of TiO₂ nanoparticle uptake, the cells with an initial density of 1.6×10^4 cells/cm² on six-well plates, seeded 15–16 h prior to the experiment, were treated with one of the following uptake inhibitor treatments for 1 h prior to the TiO₂ exposure: (1) incubated at 4 °C (instead of 37 °C), (2) addition of 50 mM sodium azide and 2-deoxy-D-glucose, (3) addition of 0.45 M sucrose, (4) addition of 50 μM nystatin, and (5) addition of 0.45 M sucrose and 50 μM nystatin.¹⁶ The cells were then incubated with 150 μg/mL final concentration of TiO₂ nanoparticles for 1 h. For the cells prepared for low-temperature treatment, the incubation was conducted at 4 °C instead of 37 °C. The treated cells were then washed with HBSS and then quantified by ICP-OES.

Toxicity Evaluation. The toxicity of nanoparticles was evaluated using four different assays to assess different biological end points: (1) CellTiter-Blue (AlamarBlue) assay to determine the cell metabolic activity; (2) MTS assay to determine the cell mitochondrial activity; and (3) CellTiter-Glo Luminescent cell viability assay to determine the level of cellular energy (ATP). For each assay, cell cultures were established at an initial cell density of 1.6×10^4 cells/cm², and the cells were exposed to different concentrations (30–3000 μg/mL) of TiO₂ for 24 h prior to evaluation.

Cell Metabolic Activity. After 24 h incubation with TiO₂ particles, the cells were washed three times with HBSS, and 20 μL of the CellTiter Blue reagent was added to each well with 100 μL of

RPMI1640 media supplemented with 1% L-glutamine only. The fluorescence signal was then quantified by measuring absorbance at excitation 544 nm and emission 590 nm using an f_{max} fluorescence plate reader (Molecular Devices) after 4 h incubation with the assay reagent.

Cell Mitochondrial Activity. After 24 h incubation with TiO₂ particles, the cells were washed three times with HBSS, and 20 μ L of MTS/PMS reagent mixture was added to each well with 100 μ L of RPMI1640 media supplemented with 1% L-glutamine only. The plate was then incubated at 37 °C for 4 h before it was quantified by measuring the absorbance at 490 nm.

Level of Cellular Energy (ATP). After 24 h incubation with TiO₂ particles, the cells were washed three times with HBSS, and 100 μ L of CellTiter-Glo Luminescent cell viability assay reagent was added to each well. The plate was then mixed using an orbital shaker for 2 min, followed by 10 min incubation to stabilize the luminescence signals. Luminescence was read using a luminometer (Turner Biosystems, model 9100-102).

Statistical Analysis. Statistical comparison of multiple groups of data was analyzed using one-way ANOVA followed by a Dunnett's test, which was used to compare means from the control group and each of the groups exposed to particles. The statistical tests were performed using the Minitab v13 statistical program (Minitab Inc.). The values are expressed as the mean \pm standard error of the mean. Statistical significance versus the control group was established as $p < 0.05$.

Conflict of Interest: The authors declare no competing financial interest.

Acknowledgment. This research was supported by the Australian Research Council through the ARC Centre of Excellence for Functional Nanomaterials (CE0348243). The authors would also like to thank the Electron Microscope and Solid State and Elemental Analysis Units at the University of New South Wales' Mark Wainwright Analytical Centre for access to their transmission electron microscope and inductively coupled plasma-optical emission spectrometer and also M. Chakravarthy for his help in particle uptake experiments shown in Figure 3.

Supporting Information Available: SDS-PAGE and Western blot analyses of serum-treated particles, microscopic evaluation of cellular attachment following particle exposure, and cell count data for uptake inhibition experiments. This material is available free of charge via the Internet at <http://pubs.acs.org>.

REFERENCES AND NOTES

- Walkey, C. D.; Olsen, J. B.; Guo, H.; Emili, A.; Chan, W. C. W. Nanoparticle Size and Surface Chemistry Determines Serum Protein Adsorption and Macrophage Uptake. *J. Am. Chem. Soc.* **2012**, *134*, 2139–2147.
- Soenen, S. J.; Rivera-Gil, P.; Montenegro, J. M.; Parak, W. J.; De Smedt, S. C.; Braeckmans, K. Cellular Toxicity of Inorganic Nanoparticles: Common Aspects and Guidelines for Improved Nanotoxicity Evaluation. *Nano Today* **2011**, *6*, 446–465.
- Vippola, M.; Falck, G. C. —M.; Lindberg, H. K.; Suhonen, S.; Vanhala, E.; Norppa, H.; Savolainen, K.; Tossavainen, A.; Tuomi, T. Preparation of Nanoparticle Dispersions for *in Vitro* Toxicity Testing. *Hum. Exp. Toxicol.* **2009**, *28*, 377–385.
- Foucaud, L.; Wilson, M. R.; Brown, D. M.; Stone, V. Measurement of Reactive Species Production by Nanoparticles Prepared in Biologically Relevant Media. *Toxicol. Lett.* **2007**, *174*, 1–9.
- Deguchi, S.; Yamazaki, T.; Mukai, S.-A.; Usami, R.; Horikoshi, K. Stabilization of C₆₀ Nanoparticles by Protein Adsorption and Its Implications for Toxicity Studies. *Chem. Res. Toxicol.* **2007**, *20*, 854–858.
- Johnston, H. J.; Semmler-Behnke, M.; Brown, D. M.; Kreyling, W.; Tran, L.; Stone, V. Evaluating the Uptake and Intracellular Fate of Polystyrene Nanoparticles by Primary and Hepatocyte Cell Lines *in Vitro*. *Toxicol. Appl. Pharmacol.* **2010**, *242*, 66–78.
- Wiogo, H. T. R.; Lim, M.; Bulmus, V.; Yun, J.; Amal, R. Stabilization of Magnetic Iron Oxide Nanoparticles in Biological Media by Fetal Bovine Serum (FBS). *Langmuir* **2011**, *27*, 843–850.
- Bastian, S.; Busch, W.; Kühnel, D.; Springer, A.; Meißner, T.; Holke, R.; Scholz, S.; Iwe, M.; Pompe, W.; Gelinsky, M.; *et al.* Toxicity of Tungsten Carbide and Cobalt-Doped Tungsten Carbide Nanoparticles in Mammalian Cells *in Vitro*. *Environ. Health Perspect.* **2009**, *117*, 530–536.
- Schulze, C.; Kroll, A.; Lehr, C. M.; Schäfer, U. F.; Becker, K.; Schnekenburger, J.; Schulze-Isfort, C.; Landsiedel, R.; Wohlleben, W. Not Ready to Use—Overcoming Pitfalls When Dispersing Nanoparticles in Physiological Media. *Nanotoxicology* **2008**, *2*, 51–61.
- Tenzer, S.; Docter, D.; Rosfa, S.; Wlodarski, A.; Kuharev, J.; Rekić, A.; Knauer, S. K.; Bantz, C.; Nawroth, T.; Bier, C.; *et al.* Nanoparticle Size Is a Critical Physicochemical Determinant of the Human Blood Plasma Corona: A Comprehensive Quantitative Proteomic Analysis. *ACS Nano* **2011**, *5*, 7155–7167.
- Maiorano, G.; Sabella, S.; Sorce, B.; Brunetti, V.; Malvindi, M. A.; Cingolani, R.; Pompa, P. P. Effects of Cell Culture Media on the Dynamic Formation of Protein–Nanoparticle Complexes and Influence on the Cellular Response. *ACS Nano* **2010**, *4*, 7481–7491.
- Cedervall, T.; Lynch, I.; Foy, M.; Berggård, T.; Donnelly, S. C.; Cagney, G.; Linse, S.; Dawson, K. A. Detailed Identification of Plasma Proteins Adsorbed on Copolymer Nanoparticles. *Angew. Chem.* **2007**, *119*, 5856–5858.
- Lynch, I.; Cedervall, T.; Lundqvist, M.; Cabaleiro-Lago, C.; Linse, S.; Dawson, K. A. The Nanoparticle-Protein Complex as a Biological Entity; a Complex Fluids and Surface Science Challenge for the 21st Century. *Adv. Colloid Interface Sci.* **2007**, *134*, 167–174.
- Lynch, I.; Dawson, K. A. Protein-Nanoparticle Interactions. *Nano Today* **2008**, *3*, 40–47.
- Alkilany, A. M.; Nagaria, P. K.; Hexel, C. R.; Shaw, T. J.; Murphy, C. J.; Wyatt, M. D. Cellular Uptake and Cytotoxicity of Gold Nanorods: Molecular Origin of Cytotoxicity and Surface Effects. *Small* **2009**, *5*, 701–708.
- Arsianti, M.; Lim, M.; Marquis, C. P.; Amal, R. Polyethylenimine Based Magnetic Iron-Oxide Vector: The Effect of Vector Component Assembly on Cellular Entry Mechanism, Intracellular Localization, and Cellular Viability. *Biomacromolecules* **2010**, *11*, 2521–2531.
- Bajaj, A.; Samanta, B.; Yan, H.; Jerry, D. J.; Rotello, V. M. Stability, Toxicity and Differential Cellular Uptake of Protein Passivated-Fe₃O₄ Nanoparticles. *J. Mater. Chem.* **2009**, *19*, 6328–6331.
- Ehrenberg, M. S.; Friedman, A. E.; Finkelstein, J. N.; Oberdörster, G.; McGrath, J. L. The Influence of Protein Adsorption on Nanoparticle Association with Cultured Endothelial Cells. *Biomaterials* **2009**, *30*, 603–610.
- Giljohann, D. A.; Seferos, D. S.; Patel, P. C.; Millstone, J. E.; Rosi, N. L.; Mirkin, C. A. Oligonucleotide Loading Determines Cellular Uptake of DNA-Modified Gold Nanoparticles. *Nano Lett.* **2007**, *7*, 3818–3821.
- Witasz, E.; Kupferschmidt, N.; Bengtsson, L.; Hultenby, K.; Smedman, C.; Paulie, S.; Garcia-Bennett, A. E.; Fadeel, B. Efficient Internalization of Mesoporous Silica Particles of Different Sizes by Primary Human Macrophages without Impairment of Macrophage Clearance of Apoptotic or Antibody-Opsonized Target Cells. *Toxicol. Appl. Pharmacol.* **2009**, *239*, 306–319.
- Chen, Z.; Xu, R.; Zhang, Y.; Gu, N. Effects of Proteins from Culture Medium on Surface Property of Silanes-Functionalized Magnetic Nanoparticles. *Nanoscale Res. Lett.* **2009**, *4*, 204–209.
- Dutta, D.; Sundaram, S. K.; Teegarden, J. G.; Riley, B. J.; Fifield, L. S.; Jacobs, J. M.; Addleman, S. R.; Kaysen, G. A.; Moudgil, B. M.; Weber, T. J. Adsorbed Proteins Influence the Biological Activity and Molecular Targeting of Nanomaterials. *Toxicol. Sci.* **2007**, *100*, 303–315.
- Kirchner, C.; Liedl, T.; Kudera, S.; Pellegrino, T.; Munoz-Javier, A.; Gaub, H. E.; Stolze, S.; Fertig, N.; Parak, W. J. Cytotoxicity of Colloidal CdSe and CdSe/ZnS Nanoparticles. *Nano Lett.* **2004**, *5*, 331–338.

24. Hauck, T. S.; Ghazani, A. A.; Chan, W. C. W. Assessing the Effect of Surface Chemistry on Gold Nanorod Uptake, Toxicity, and Gene Expression in Mammalian Cells. *Small* **2008**, *4*, 153–159.
25. Sager, T. M.; Porter, D. W.; Robinson, V. A.; Lindsley, W. G.; Schwegler-Berry, D. E.; Castranova, V. Improved Method to Disperse Nanoparticles for *in Vitro* and *in Vivo* Investigation of Toxicity. *Nanotoxicology* **2007**, *1*, 118–129.
26. Clift, M. J. D.; Bhattacharjee, S.; Brown, D. M.; Stone, V. The Effects of Serum on the Toxicity of Manufactured Nanoparticles. *Toxicol. Lett.* **2010**, *198*, 358–365.
27. Lundqvist, M.; Stigler, J.; Elia, G.; Lynch, I.; Cedervall, T.; Dawson, K. A. Nanoparticle Size and Surface Properties Determine the Protein Corona with Possible Implications for Biological Impacts. *Proc. Natl. Acad. Sci. U. S. A.* **2008**, *105*, 14265–14270.
28. Vesaratchanon, S.; Nikolov, A.; Wasan, D. T. Sedimentation in Nano-Colloidal Dispersions: Effects of Collective Interactions and Particle Charge. *Adv. Colloid Interface Sci.* **2007**, *134*, 268–278.
29. Tedja, R.; Marquis, C.; Lim, M.; Amal, R. Biological Impacts of TiO₂ on Human Lung Cell Lines A549 and H1299: Particle Size Distribution Effects. *J. Nanopart. Res.* **2011**, *13*, 3801–3813.
30. Wittmaack, K. Excessive Delivery of Nanostructured Matter to Submersed Cells Caused by Rapid Gravitational Settling. *ACS Nano* **2011**, *5*, 3766–3778.
31. Dombu, C. Y.; Kroubi, M.; Zibouche, R.; Matran, R.; Betbeder, D. Characterization of Endocytosis and Exocytosis of Cationic Nanoparticles in Airway Epithelium Cells. *Nanotechnology* **2010**, *21*, 355102–355109.
32. Panyam, J.; Labhasetwar, V. Dynamics of Endocytosis and Exocytosis of Poly (D, L-Lactide-Co-Glycolide) Nanoparticles in Vascular Smooth Muscle Cells. *Pharm. Res.* **2003**, *20*, 212–220.
33. Torchilin, V. P.; Rammohan, R.; Weissig, V.; Levchenko, T. S. Tat Peptide on the Surface of Liposomes Affords Their Efficient Intracellular Delivery Even at Low Temperature and in the Presence of Metabolic Inhibitors. *Proc. Natl. Acad. Sci. U. S. A.* **2001**, *98*, 8786–8791.
34. Kim, J. S.; Yoon, T. J.; Yu, K. N.; Noh, M. S.; Woo, M.; Kim, B. G.; Lee, K. H.; Sohn, B. H.; Park, S. B.; Lee, J. K. Cellular Uptake of Magnetic Nanoparticle is Mediated Through Energy Dependent Endocytosis in A549 Cells. *J. Vet. Sci.* **2006**, *7*, 321–326.
35. Heuser, J. E.; Anderson, R. G. Hypertonic Media Inhibit Receptor-Mediated Endocytosis by Blocking Clathrin-Coated Pit Formation. *J. Cell Biol.* **1989**, *108*, 389–400.
36. Li, W.; Chen, C.; Ye, C.; Wei, T.; Zhao, Y.; Lao, F.; Chen, Z.; Meng, H.; Gao, Y.; Yuan, H.; *et al.* The Translocation of Fullerene Nanoparticles into Lysosome via the Pathway of Clathrin-Mediated Endocytosis. *Nanotechnology* **2008**, *19*, 145102–145114.
37. Kam, N. W. S.; Dai, H. Carbon Nanotubes As Intracellular Protein Transporters: Generality and Biological Functionality. *J. Am. Chem. Soc.* **2005**, *127*, 6021–6026.
38. Khalil, I. A.; Kogure, K.; Akita, H.; Harashima, H. Uptake Pathways and Subsequent Intracellular Trafficking in Non-viral Gene Delivery. *Pharmacol. Rev.* **2006**, *58*, 32–45.
39. Chen, Y.; Wang, S.; Lu, X.; Zhang, H.; Fu, Y.; Luo, Y. Cholesterol Sequestration by Nystatin Enhances the Uptake and Activity of Endostatin in Endothelium via Regulating Distinct Endocytic Pathways. *Blood* **2011**, *117*, 6392–6403.
40. Taylor, D. R.; Watt, N. T.; Perera, W. S. S.; Hooper, N. M. Assigning Functions to Distinct Regions of the N-Terminus of the Prion Protein That are Involved in Its Copper-Stimulated, Clathrin-Dependent Endocytosis. *J. Cell Sci.* **2005**, *118*, 5141–5153.
41. Preissner, K. T. Structure and Biological Role of Vitronectin. *Annu. Rev. Cell Biol.* **1991**, *7*, 275–310.
42. Boylan, A. M.; Sanan, D. A.; Sheppard, D.; Broaddus, V. C. Vitronectin Enhances Internalization of Crocidolite Asbestos by Rabbit Pleural Mesothelial Cells via the Integrin Alpha v Beta 5. *J. Clin. Invest.* **1995**, *96*, 1987–2001.
43. Pande, P.; Mosleh, T. A.; Aust, A. E. Role of [Alpha]_v[Beta]₅ Integrin Receptor in Endocytosis of Crocidolite and Its Effect on Intracellular Glutathione Levels in Human Lung Epithelial (A549) Cells. *Toxicol. Appl. Pharmacol.* **2006**, *210*, 70–77.
44. Lin, J.; Zhang, H.; Chen, Z.; Zheng, Y. Penetration of Lipid Membranes by Gold Nanoparticles: Insights into Cellular Uptake, Cytotoxicity, and Their Relationship. *ACS Nano* **2010**, *4*, 5421–5429.
45. Mahmoudi, M.; Laurent, S.; Shokrgozar, M. A.; Hosseinkhani, M. Toxicity Evaluations of Superparamagnetic Iron Oxide Nanoparticles: Cell Vision Versus Physicochemical Properties of Nanoparticles. *ACS Nano* **2011**, *5*, 7263–7276.
46. Laurent, S.; Burtea, C.; Thirifays, C.; Häfeli, U. O.; Mahmoudi, M. Crucial Ignored Parameters on Nanotoxicology: The Importance of Toxicity Assay Modifications and “Cell Vision”. *PLoS One* **2012**, *7*, e2999710.1371/journal.pone.0029997.
47. Zhu, Y.; Li, W.; Li, Q.; Li, Y.; Li, Y.; Zhang, X.; Huang, Q. Effects of Serum Proteins on Intracellular Uptake and Cytotoxicity of Carbon Nanoparticles. *Carbon* **2009**, *47*, 1351–1358.
48. Bickley, R. I.; Gonzalez-Carreno, T.; Lees, J. S.; Palmisano, L.; Tilley, R. J. D. A Structural Investigation of Titanium Dioxide Photocatalysts. *J. Solid State Chem.* **1991**, *92*, 178–190.